Available online at www.sciencedirect.com
ScienceDirect
Polymer 48 (2007) 1651–1658
polymer
www.elsevier.com/locate/polymer

Structure and dynamic mechanical properties of poly(ethylene terephthalate-*co*-4,4′-bibenzoate) fibers

Hongming Ma [a,1], David M. Collard [a], David A. Schiraldi [c], Satish Kumar [b,*]

[a] *School of Chemistry and Biochemistry, Georgia Institute of Technology, Atlanta, GA 30332-0400, USA*
[b] *School of Polymer, Textile and Fiber Engineering, Georgia Institute of Technology, Atlanta, GA 30332-0295, USA*
[c] *Department of Macromolecular Science and Engineering, Case Western Reserve University, Cleveland, OH 44106, USA*

Received 3 August 2006; received in revised form 13 January 2007; accepted 15 January 2007
Available online 19 January 2007

Abstract

Poly(ethylene terephthalate-*co*-4,4′-bibenzoate) (PETBB) fibers containing 5, 15, 35, 45, 55, and 65 mol% bibenzoate (BB) were melt spun. Fiber structure has been determined using wide angle X-ray diffraction, birefringence, and FTIR spectroscopy. When drawn to their respective maximum draw ratios, the structures and properties of high BB containing fibers (PETBB45, 55 and 65) are significantly different than those of PET and low BB containing fibers (PETBB5, 15, and 35). For example, 90% of the ethylene glycol units in high BB containing fibers are in the *trans* conformation, while only 80% of these units are in *trans* conformation in PET and low BB containing fibers. Overall orientation of the high BB containing fibers is higher (orientation factor $f > 0.85$) than those of PET and low BB containing fibers ($f < 0.6$). Orientation of the crystalline regions is quite high ($f_{cr} \sim 0.95$) for both groups of fibers, while orientation of the amorphous regions (f_{am}) of high BB containing fibers is higher ($\sim$0.8) than those of the PET and low BB containing fibers ($\sim$0.4). High BB containing fibers exhibit much higher storage modulus and modulus retention with temperature than low BB containing fibers. Glass transition temperature determined from the dynamic loss tangent peak decreased with increasing BB content, while this transition completely disappeared in the high BB containing fibers. The magnitude of the secondary transition, observed at about −50 °C, decreased with increasing BB content. Another secondary transition, not observed in PET, was observed at about 70 °C in high BB containing fibers. These dynamic mechanical results have been rationalized in terms of the observed structural parameters.

Keywords: Wide angle X-ray diffraction; Fourier transform infrared spectroscopy; Poly(ethylene terephthalate-*co*-4,4′-bibenzoate)

1. Introduction

High performance fibers and films can be processed from poly(ethylene terephthalate-*co*-4,4′-bibenzoate) (PETBB) random copolymers [1–3]. PETBB fibers with 45, 55, and 65 mol% bibenzoate (BB) exhibit tensile modulus values in the range of 35–45 GPa, which is approaching the value for thermotropic liquid crystalline *co*-polyesters [4]. Homopolymers of 4,4′-bibenzoate and various diols have been shown to be liquid crystalline [5,6]. Transient liquid crystallinity has been reported in PET [7–10] and its copolymer with poly(ethylene naphthalate) [11]. The unique spinning behavior of PETBB45, 55, and 65, that highly oriented fiber can be obtained at relatively low speed, indicates the possibility of the formation of a shear-induced liquid crystalline phase. By comparison, the modulus of PET and low BB containing PETBB fibers is only about 10 GPa. High BB containing fibers also have much better modulus retention at elevated temperature than PET and low BB containing fibers. Crystal structure of PETBB15 and 35 is similar to that of PET, while PETBB45, 55, and 65 have the crystal structure of poly(ethylene bibenzoate) (PEBB) homopolymer [1,12,13]. Structural and dynamic mechanical properties of low and high BB containing fibers are presented and discussed in this paper.

* Corresponding author. Tel.: +1 404 894 7550.
E-mail address: satish.kumar@gatech.edu (S. Kumar).
[1] Present address: The Dow Chemical Company, Freeport, TX, USA.

0032-3861/$ - see front matter © 2007 Elsevier Ltd. All rights reserved.
doi:10.1016/j.polymer.2007.01.026

2. Experimental

Synthesis of (PETBB) copolymers used in this study has been reported elsewhere [1,14]. Intrinsic viscosities (measured in dichloro acetic acid at 25 °C) for PET, PETBB15, 35, 45, 55, and 65 were 0.90, 0.94, 0.88, 0.92, 0.92, and 0.90 dl/g, respectively. Fibers were melt spun at temperature range of 270–310 °C and were drawn to their maximum achievable draw ratios. Fiber spinning was carried out using a small-scale piston driven melt spinning system manufactured by Bradford Research Limited using a 250 μm diameter spinneret. Polymer samples were dried in vacuum at 80 °C for at least 2 days prior to spinning. Fiber take up speed was in the range of 100–400 m/min. As spun fibers PETBB45, 55, and 65 were fully drawn to begin with, while as spun PET, PETBB5, 15, and 35 were subsequently drawn on a hot plate at 120 °C. All fibers were heat treated at constant length at 150 °C for 10 min. Birefringence was measured using the Leitz Ortholux polarizing microscope and a Zeiss compensator. The spinning temperatures, achievable draw ratios, fiber tensile modulus, and birefringence are listed in Table 1. Fiber diameter in all cases was about 15 μm. For further fiber spinning details, reader could refer to Ref. [15].

X-ray diffraction was carried out on multifilament bundles on a Rigaku small/wide angle X-ray scattering system with a MicroMax 002™ X-ray beam generator operating at 45 kV and 0.66 mA. Cu Kα irradiation was obtained using confocal Max-Flux® optics. 2D diffraction images were collected using a Rigaku R-AXIS IV^{++} detector. Radial, equatorial, and azimuthal scans were integrated using AreaMax® software and profile fittings were carried out using MDI Jade 6.1. A linear background was fitted for all the curves. Crystallinity was obtained from the ratio of the integrated intensity of the crystalline peaks to that of the total integrated intensity. The crystalline and amorphous fitted peaks are shown in Fig. 1 for PET, low BB, and high BB containing PETBB fibers. Crystallite size was measured using the Scherrer's equation [16]. Crystallite orientation was measured from the azimuthal scans. For PET and low BB containing fibers, with a triclinic unit cell, Herman's c-axis orientation factor [17], f_c, was determined using Eq. (1).

$$f_c = 1 - \frac{3}{2}\langle \sin^2\theta \rangle \tag{1}$$

Table 1
Fiber processing conditions and physical properties[a]

Polymer	T_m (°C)	Spinning temperature (°C)	Draw ratio[b]	Tensile modulus (GPa)	Birefringence
PET	260	280	6	12 ± 2	0.18
PETBB15	245	270	4	10 ± 2	0.21
PETBB35	230	270	3	9 ± 3	0.26
PETBB45	245	290	ND	38 ± 3	0.36
PETBB55	275	300	ND	40 ± 5	0.45
PETBB65	290	310	ND	45 ± 4	0.40

ND: non drawn fiber.
[a] All fibers were heat treated at constant length at 150 °C for 10 min.
[b] Fibers were drawn on a hot plate set at 120 °C.

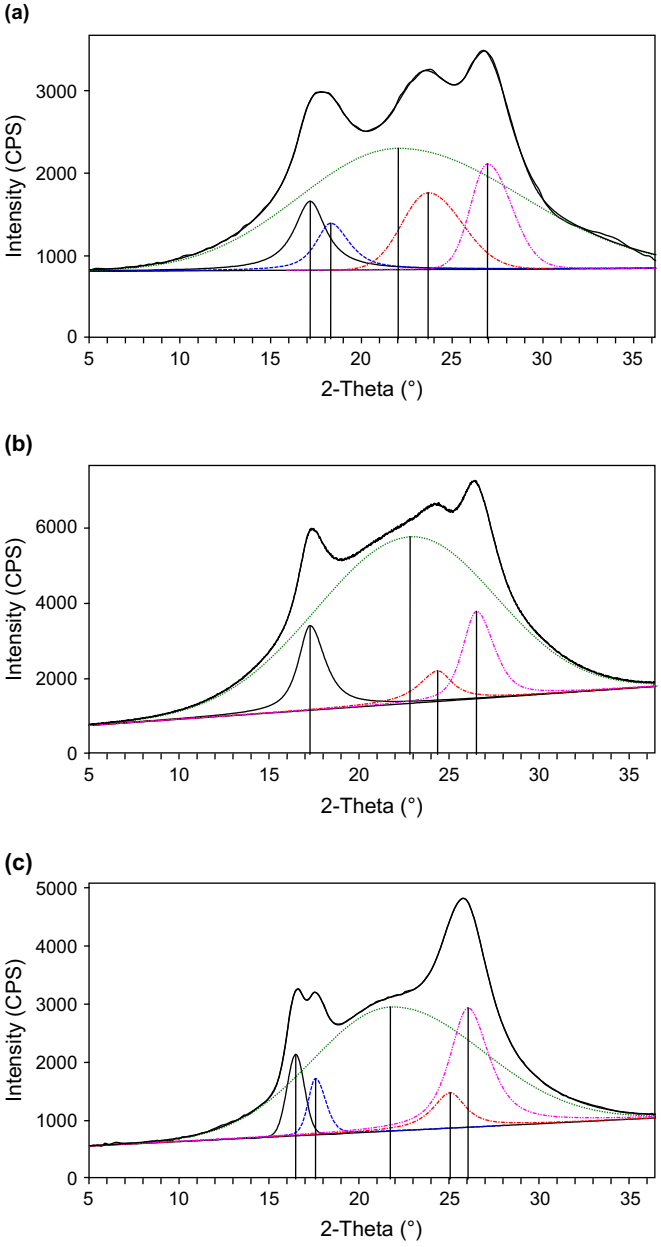

Fig. 1. Curve fitted wide angle X-ray diffraction radial scans of (a) PET, (b) PETBB35, and (c) PETBB55.

where θ is the angle between the fiber axis and polymer chain axis (c-axis).

For PET and low BB containing fibers, $\langle \sin^2\theta \rangle$ was determined using (010), (1$\bar{1}$0), and (100) azimuthal peaks and Eq. (2).

$$\langle \sin^2\theta \rangle = 0.356\left\langle \cos^2\phi_{(010),Z} \right\rangle + 0.767\left\langle \cos^2\phi_{(1\bar{1}0),Z} \right\rangle + 0.877\left\langle \cos^2\phi_{(100),Z} \right\rangle \tag{2}$$

where ϕ is the angle between the given plane normal and the fiber axis (z). Values of $\langle \cos^2\phi \rangle$ were determined from the respective azimuthal wide angle X-ray diffraction scans. For the high BB containing fibers, the unit cell parameters [12]

are $a = 5.75$, $b = 3.82$, $c = 14.62$, $\alpha = 90.1°$, $\beta = 90.3°$ and $\gamma = 78.1°$ and the cell is almost monoclinic as $\alpha \approx \beta \approx 90°$. For high BB containing fibers, a-axis orientation (f_a) was determined from (100) peak. Using the orthogonality condition [18] for the monoclinic cell, c-axis orientation was determined using $f_c = -2f_a$. Overall molecular orientation in the fiber (f_{fiber}) was determined based on the two phase approximation using Eq. (3).

$$f_{\text{fiber}} = f_{\text{cr}}V_{\text{cr}} + f_{\text{am}}(1 - V_{\text{cr}}) \tag{3}$$

where f_{cr} and f_{am} are orientations of crystalline and amorphous regions and V_{cr} is the volume fraction of the crystalline regions.

Orientation for all the fibers was also determined using infrared dichroic ratio [19] D ($=A_{\parallel}/A_{\perp}$) using Eq. (4).

$$f = \frac{D-1}{D+2} \times \frac{D_0+2}{D_0-1} \tag{4}$$

where $A_{\parallel}$ and $A_{\perp}$ are the infrared absorption peak areas with beam polarized parallel and perpendicular to the fiber axis. The intrinsic dichroic ratio (D_0) of a perfectly oriented sample is given by $D_0 = 2\cot^2\alpha$, where α is the transition moment angle; that is the angle between the polymer chain axis and the transition moment direction of the vibrational mode. FTIR spectra of the fibers were obtained on a Perkin Elmer Spectrum One FTIR spectrometer. IR spectra were collected in the transmission mode at 4 cm^{-1} resolution with the beam polarized parallel and perpendicular to the fiber axis.

Dynamic mechanical measurements were made on 20 filament bundles at a gage length of 20 mm on a Seiko DMS (Model 220). A static stress of ~10 MPa and dynamic strain of 0.1% was applied for these tests. Activation energy was calculated using Arrhenius equation [20].

3. Results and discussion

Modulus of PET and low BB containing fibers is in the range of 9–12 GPa, while for high BB containing fibers it is in the range of 38–45 GPa. The birefringence of BB containing fibers is as high as 0.45. The addition of bibenzoate copolymer disrupts PET crystallinity. Even PETBB45 and 55 exhibiting high modulus have significantly lower crystallinity than PET. Data in Table 2 show that the transverse crystallite size in PET and low BB containing fibers is significantly smaller (about 4 nm × 6 nm) than in high BB containing fibers (about 4 nm × 10 nm).

Table 2
Crystallinity, crystallite size, and orientation in various fibers

Fiber	Crystallinity (wt%)	Crystal size (nm)		f_{cr}	f_{am}	f_{fiber}
		(010)	(100)			
PET	41	5.6	3.8	0.95	0.39	0.60
PETBB15	37	6.0	4.0	0.94	0.33	0.54
PETBB35	21	4.8	4.5	0.95	0.34	0.52
PETBB45	23	4.2	9.2	0.98	0.84	0.86
PETBB55	32	3.8	9.6	0.97	0.83	0.88
PETBB65	43	4.1	10.0	0.98	0.86	0.91

FTIR spectra of drawn and heat-treated PET and PETBB fibers (Fig. 2) show that absorbance corresponding to C=O stretch at 1730 cm^{-1}, COO stretch at around 1260 cm^{-1}, and COC stretch at 1120 cm^{-1} in the spectra of PETBB are all similar to those observed in PET. In PETBB, new absorbance peaks are observed at 1560, 1401, 1008, 845, 780 and 760 cm^{-1} arising from bibenzoate units. Aromatic ring orientation is determined from aromatic C–H bending or stretching vibrations. The in-plane bending absorbance in the phenyl ring at 1018 cm^{-1} and in biphenyl ring at 1008 cm^{-1} gives the overall orientations of the terephthalate (T) and bibenzoate (BB) units, respectively. The reported transition moment angle of this transition is 20° [21], and the resulting orientation factor for phenyl rings in PET fiber is 0.6 (Table 3). The phenyl ring orientation in low BB containing fibers is lower (0.56 and 0.54) and in high BB containing fibers (PETBB45, 55 and 65) it is higher (0.79–0.84) than that for PET. For the biphenyl moiety, assuming the same transition moment angle of 20°, similar orientation trends are observed in low and high BB containing fibers. However, for low BB containing fibers, the BB orientation is lower than the T orientation, while for high BB containing fibers, BB orientation is higher than the T orientation (Table 3). A strong peak at 730 cm^{-1} in PET arises due to out-of-plane C–H bending from benzene ring with a transition moment angle close to 90° [24]. This peak is too strong to be used for orientation analysis for the control PET fiber. However in high BB containing polymers this peak has moderate intensity due to the reduced concentration of T units. The C–H out-of-plane bending from the BB moiety is observed at 756 cm^{-1}. Orientations of the T and BB units calculated from 730 and 756 cm^{-1} bands, respectively, are also listed in Table 3. While the absolute T and BB orientation values obtained from in-plane bending mode and out-of-plane bending mode differ from each other, the trends represented by the two sets of values are the same; that is orientation of BB and T units are higher in high BB containing fibers than in PET and low BB containing fibers.

FTIR dichroism also allows for the orientation determination of the terephthalate units only in the amorphous region using 1579 cm^{-1} peak characteristic of 1,4 para–para ring stretching mode V_{8A} [22]. Due to the centro-symmetric nature, this vibration is only Raman-active in the crystalline regions [23]. However, it is IR-active in the amorphous regions, as the C=O adjacent to the ring rotates out of the plane of the ring, and the OC–Phenyl–CO segment deviates from coplanarity, thereby, breaking the centro-symmetry. Thus, this peak is characteristic of the amorphous regions [24,25]. In the 4,4′-bibenzoate unit this vibration appears at 1560 cm^{-1}, and as expected FTIR spectra of PETBB fibers show two peaks in the range of 1600–1540 cm^{-1} (Fig. 3). The fact that 1579 cm^{-1} peak is from terephthalate and 1560 cm^{-1} peak is from bibenzoate was confirmed from the FTIR spectra of dimethyl terephthalate and dimethyl 4,4′-bibenzoate model compounds. Dichroic ratios (D) of these bands (Table 4) confirm high orientation of T and BB units in the amorphous

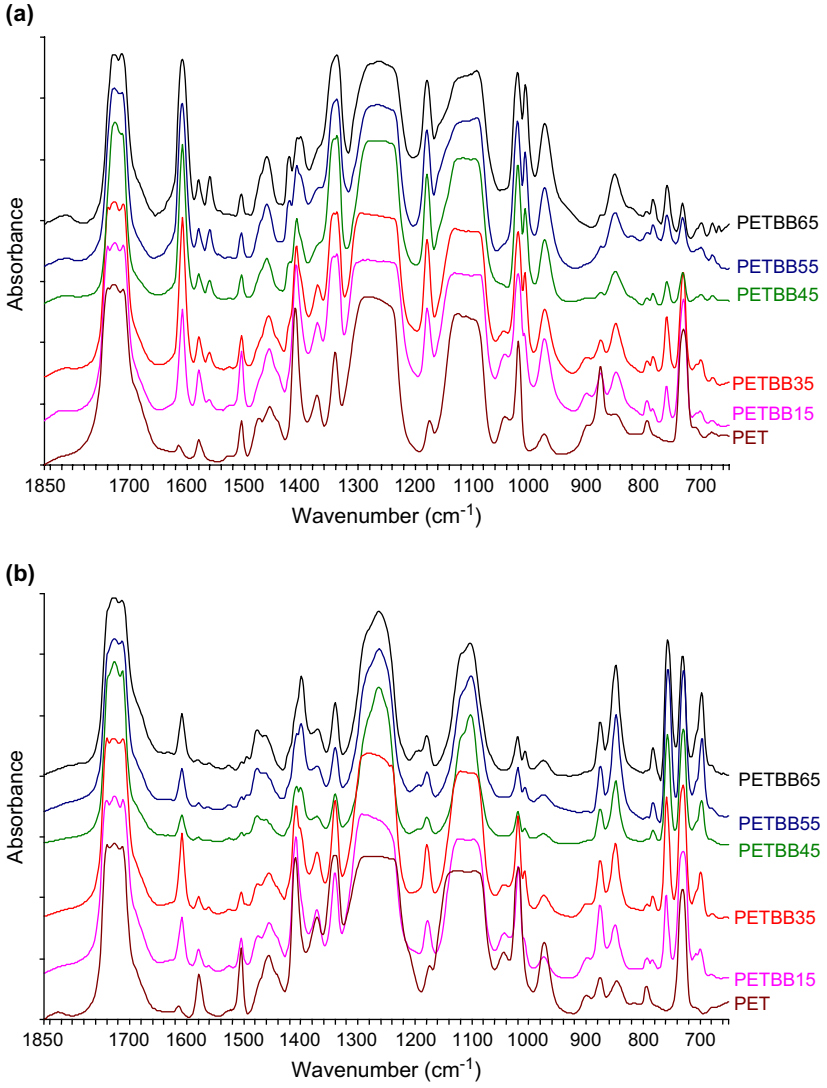

Fig. 2. FTIR spectra of various fibers with polarization direction: (a) parallel and (b) perpendicular to the fiber axis.

regions of high BB containing fibers. However, due to lack of information on the transition moment angles, the Herman's orientation factors of these bands were not calculated.

The ethylene unit in the amorphous [23] regions can adopt either *trans* or *gauche* conformation and give different absorption peaks corresponding to CH_2 wagging: absorption peaks due to *trans* conformation is observed at 1340 cm^{-1} and for *gauche* at 1370 cm^{-1} (Fig. 4). In the crystalline region they only adopt *trans* conformation. Based on the relative peak areas of the two conformations, the percentage of *trans* conformations observed is listed in Table 5. In PET and low BB containing fibers, about 80% of the ethylene units are in *trans* conformation, while in high BB containing fibers, the percentage of *trans* conformations is above 90%. Taking into account the crystallinity determined from X-ray diffraction, the percentage of *trans* conformers in the amorphous regions was also calculated (Table 5). Approximately 85% of the ethylene units in the amorphous regions of high BB containing fibers are in the *trans* conformation, while in PET and low BB containing fibers this value is only 65%. Orientation of the *trans* conformers obtained from 1340 cm^{-1} ($\alpha = 21°$ [26]) and 973 cm^{-1} (*trans* glycol C–O stretching, $\alpha = 4°$ [26]) peaks is high (0.85–0.90) in the high BB containing fibers and rather low (0.5–0.6) in low BB containing fibers. These results suggest that not only more chains in high BB containing fibers are extended, but they also have higher orientation.

Table 3
Orientation of phenyl and biphenyl rings in various fibers

Fiber	f_{1018} (C–H in-plane bending of T)	f_{1008} (C–H in-plane bending of BB)	f_{730} (C–H out-of-plane bending of T)	f_{756} (C–H out-of-plane bending of BB)
PET	0.60	–	–	–
PETBB15	0.56	0.33	–	0.55
PETBB35	0.54	0.48	0.46	0.67
PETBB45	0.79	0.93	0.68	0.88
PETBB55	0.82	0.92	0.69	0.90
PETBB65	0.84	0.94	0.67	0.92

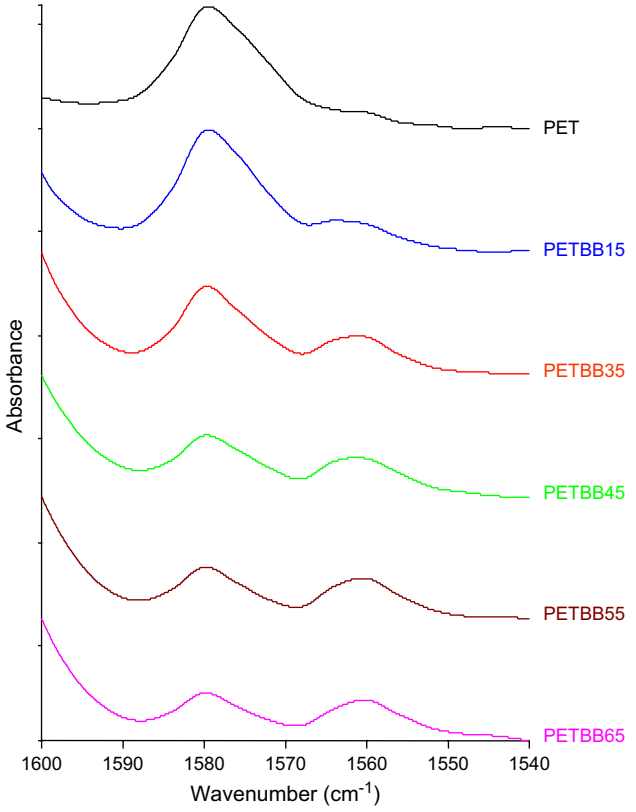

Fig. 3. FTIR spectra of various fibers in the range of 1600–1540 cm^{-1}.

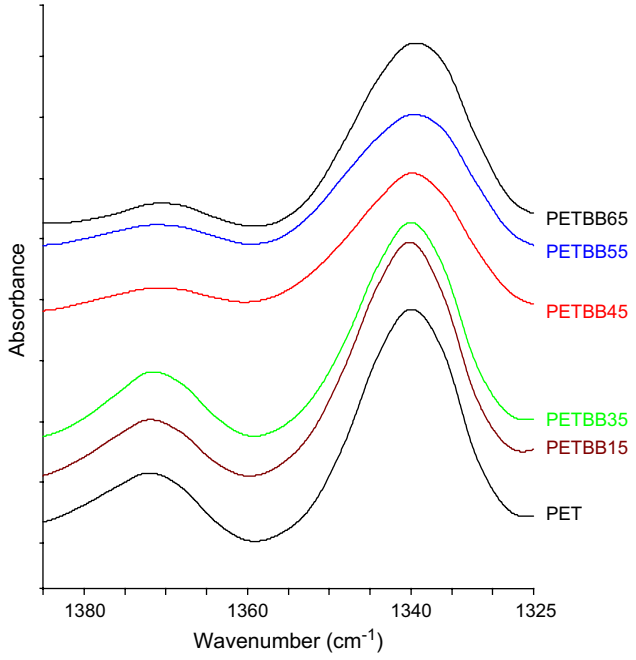

Fig. 4. FTIR spectra of various fibers in the range of 1400–1300 cm^{-1}.

The overall molecular orientation based on the orientations of the T and BB units (Table 5) and their respective concentration was calculated using Eq. (5).

$$f_{\text{fiber}} = f_T X_T + f_B X_B \quad (5)$$

where f_T, f_B and X_T, X_B are the orientation factors and mole fractions of T and B units, respectively. The orientation in the amorphous regions was determined using Eq. (3) with the overall orientation obtained from Eq. (5) and the orientation of the crystalline region f_{cr} obtained from X-ray analysis. The crystalline, amorphous, and overall orientation values are listed in Table 2. The overall and amorphous orientations of high BB containing fibers are much higher than the respective orientation values for PET and low BB containing fibers, while the crystalline orientation values in the two groups of fibers are quite comparable. Orientation of amorphous regions (f_a) for PET and low BB containing fibers is below 0.4, while in that of all high BB containing fibers it is above 0.8. Perhaps this is the most significant difference between the structures of these two groups of fibers.

Storage modulus (E') of high BB containing fibers is significantly higher and they have better modulus retention with temperature than PET and low BB containing fibers (Fig. 5). PET and low BB containing fibers exhibit glass transition tan (δ) peak in the temperature range of 120–140 °C (Fig. 6a), while this peak is not observed in the high BB containing fibers (Fig. 6b). The glass transition temperature of bulk PETBB, as measured by differential scanning calorimeter (DSC), increases with the increasing BB mole fraction [1]. However, the dynamic mechanical tan (δ) peak arising from the glass transition occurs at progressively lower temperature when BB content is increased up to 35 mol%, and at higher BB content fibers, this peak is not observed at all. The amorphous regions in PET and low BB containing fibers have low orientation ($f_a \sim 0.4$) and high percentage of ethylene units are in *gauche* conformation. This accounts for the presence of distinct glass transition. On the other hand, the amorphous regions of high BB containing fibers have a relatively low fraction of ethylene glycol units in the *gauche* conformation, and the amorphous regions are highly aligned ($f_a \sim 0.85$). Lower

Table 4
Dichroic ratio (D) of 1579 cm^{-1} and 1560 cm^{-1} peaks in various fibers

Fiber	D_{1579}	D_{1560}
PET	2.2	–
PETBB15	2.4	4.48
PETBB35	2.3	4.43
PETBB45	7.1	16.1
PETBB55	7.3	15.2
PETBB65	7.7	16.6

Table 5
Ethylene glycol *trans* conformer fraction and orientation of the *trans* conformer

Fiber	Total *trans* fraction	*trans* Fraction in amorphous regions	$f_{trans\text{-}1340}$	$f_{trans\text{-}972}$
PET	0.80	0.64	0.65	0.64
PETBB15	0.81	0.65	0.47	0.58
PETBB35	0.78	0.65	0.47	0.58
PETBB45	0.90	0.85	0.86	0.89
PETBB55	0.90	0.84	0.85	0.91
PETBB65	0.92	0.86	0.85	0.90

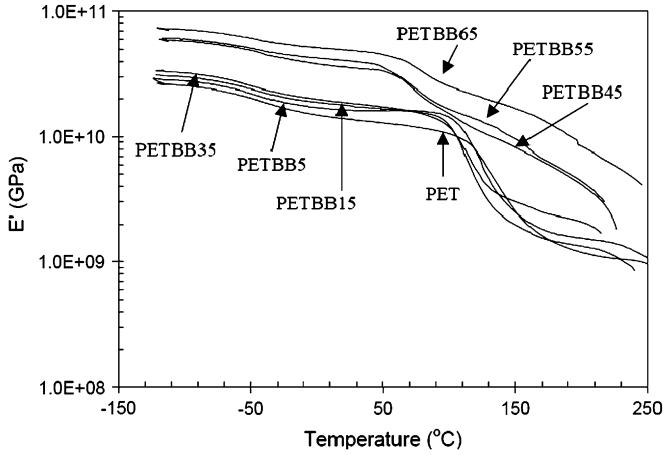

Fig. 5. Storage modulus (E') of various fibers at 10 Hz.

crystallinity and lower amorphous orientation of PETBB15 as compared to PET would be responsible for the lower tan (δ) peak temperature for the former.

In high BB containing fibers (Fig. 6b) a new tan (δ) peak appears at about 80 °C with the tan (δ) magnitude of ~0.05. This transition temperature is lower than the glass transition temperature measured for the corresponding bulk polymer

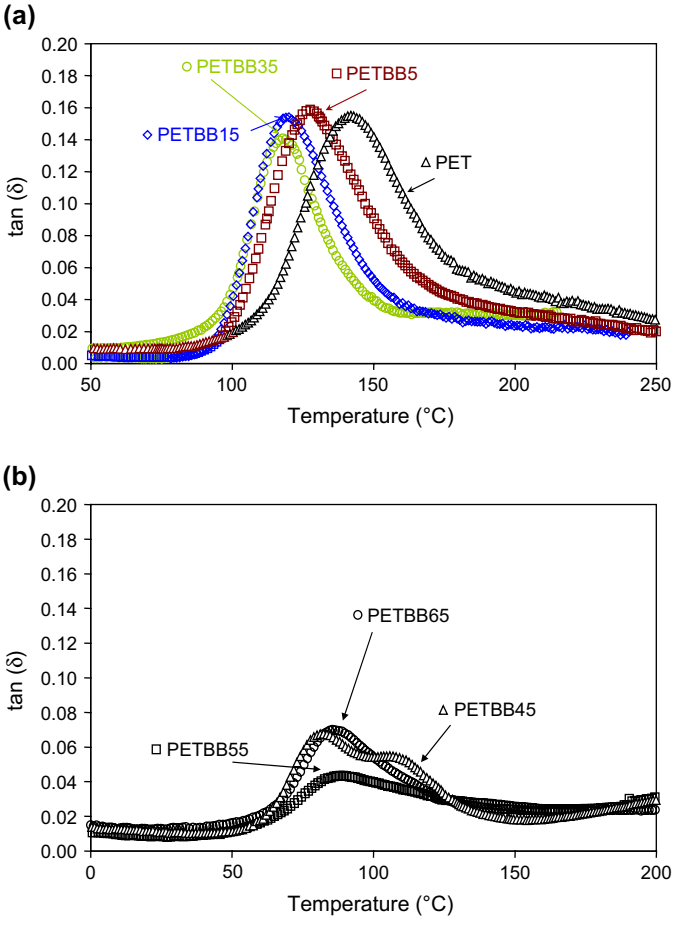

Fig. 6. Tan (δ) behavior of various fibers at 10 Hz: (a) low BB containing fibers and (b) high BB containing fibers.

Table 6
Dynamic mechanical loss transition temperatures in various fibers

Fiber	Transition temperatures (°C) at 0.1, 1, and 10 Hz		
	β_1	β_2	α
PET	−62, −51, −38		133, 138, 144
PETBB5	−59, −49, −39		118, 123, 129
PETBB15	−60, −49, −39		109, 114, 119
PETBB35	−60, −51, −41		108, 114, 119
PETBB45	−60, −52, −42	75, 78, 82	96, 101, 106
PETBB55	−62, −53, −43	78, 84, 89	–
PETBB65	−63, −55, −45	78, 82, 88	–

by DSC. It has also been shown [1] that an unoriented amorphous PETBB55 fiber shows a glass transition tan (δ) peak (magnitude ~0.5) at ~120 °C and a secondary peak (magnitude ~0.05) at ~80 °C. The glass transition peak at 120 °C completely disappears in the oriented and crystalline fiber, while the secondary peak at 80 °C is still present, and there is no change in its magnitude or temperature. The peak at 80 °C cannot be attributed to the main chain motion (glass transitions). We term this transition as a sub-T_g transition (β_2). This peak may be due to the motion of the bibenzoate units similar to that of the terephthalate units in PET at about −50 °C, which we termed as β_1 transition. Amorphous regions of the high BB containing fibers are highly extended and oriented (also see Table 2) so that the macroscopic main chain motion associated with T_g does not occur in these fibers. The loss of main chain motion is responsible for much improved modulus retention at elevated temperatures for high BB containing fibers.

Various transition temperatures and the activation energies calculated using Arrhenius equation are listed in Tables 6 and 7, respectively. The β_1 relaxation is present in all the fibers (Fig. 7) and has about the same activation energy. The β_2 relaxation is observed in high BB containing fibers and has much higher activation energy than that of β_1. The activation energy of the α relaxation in the low BB containing fibers has values typical of the PET fiber. Magnitude of the β_1 relaxation peak decreased with increasing BB content. While discussing about this peak, Ward [27] wrote, "In PET the effect of crystallinity on the β relaxation is very small and has led to a very complex interpretation in terms of this loss peak being composed of several relaxation processes." While this peak has been studied for over half a century, its origins are still a subject of active research [28–32]. As the β relaxation in PET is

Table 7
Activation energies of dynamic loss peaks in various fibers

Fiber	Activation energy (kcal/mol)		
	β_1	β_2	α
PET	18	–	140
PETBB5	20	–	140
PETBB15	20	–	140
PETBB35	21	–	141
PETBB45	22	102	123
PETBB55	23	104	–
PETBB65	23	103	–

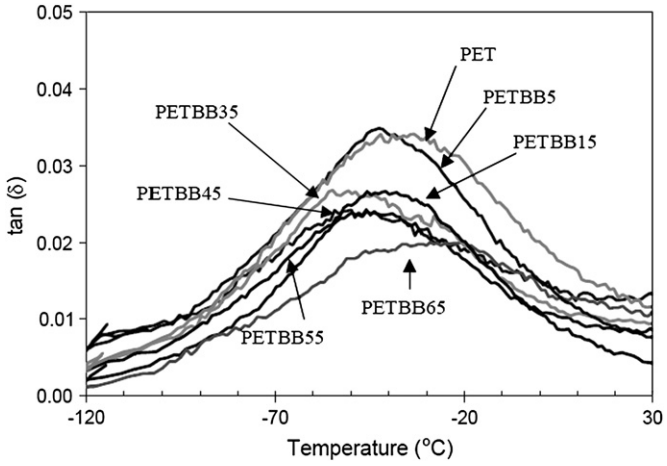

Fig. 7. β_1 Relaxation of various fibers at 10 Hz.

not significantly affected with crystallinity, it appears that this relaxation (β_1) in PETBB fibers is also not affected by the degree of crystallinity and orientation. Peak area ratio of this transition from PETBB to PET (A/A_0) is plotted as a function of BB mole fraction (Fig. 8). The peak area decreases linearly with increasing bibenzoate content suggesting that the motion contributing to this transition only involves the terephthalate moieties and not the bibenzoate moieties. The fact that β_1 relaxation in PETBB is of reduced magnitude and β_2 relaxation is observed at much higher temperature than the corresponding relaxation in PET may serve to explain the superior gas transport barrier properties of PETBB copolymer over PET [2].

4. Conclusions

Drawn and heat-treated PET exhibited good crystallinity (41%) and low modulus (12 GPa), PETBB35 exhibited low crystallinity (21%) and low modulus (9 GPa), PETBB45 exhibited low crystallinity (23%) and high modulus (38 GPa), and PETBB65 has high crystallinity (43%) and high modulus (45 GPa). Crystalline orientation in all the fibers is quite comparable, with orientation factors in the range of 0.94–0.98. However, the amorphous orientation in PET and low BB content PETBB fibers is rather low (orientation factor 0.34–0.39), while amorphous orientation in PETBB45, 55, and 65 is quite good (orientation factor 0.83–0.86). In high and low BB containing fibers, the overall percentage of *trans* conformer conforming ethylene units is 90 and 80%, while the *trans* conformers in the amorphous regions in these two groups of fibers are 85 and 65%, respectively. High BB containing fibers have significantly higher overall orientation ($f = 0.85$) than PET and low BB content fibers ($f = 0.6$). The differences in modulus between these two groups of fibers can be understood based on their orientation rather than crystallinity. High BB containing fibers also have much higher storage modulus and modulus retention at elevated temperatures than PET and low BB content fibers. The temperature at which tan (δ) glass transition peak is observed initially decreases with increasing BB content and completely disappears at high BB content. The decrease in dynamic mechanical glass transition temperature with the addition of rigid moiety (BB) is the result of decreased crystallinity (from 41 to 21%) and decreased amorphous orientation (from 0.39 to 0.34). The loss peak associated with the glass transition is nearly suppressed in PETBB45, though this sample has rather low crystallinity (23%). This is primarily a result of high amorphous orientation. The magnitude of β_1 relaxation decreases with increasing BB content. A sub-T_g transition (β_2) is also observed in high BB containing fiber, and is attributed to the motion of the bibenzoate units.

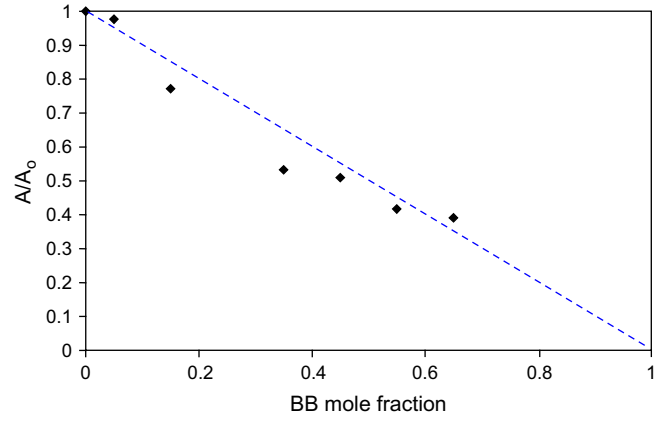

Fig. 8. β_1 Peak area ratio of PETBB (A) and PET (A_0) as a function of BB mole fraction.

Acknowledgment

Funding for this work was provided by KoSa. Assistance of Rahul Jain in preparing this manuscript is gratefully acknowledged.

References

[1] Ma H, Hibbs M, Collard DM, Kumar S, Schiraldi DA. Macromolecules 2002;35:5123.
[2] Liu RYF, Schiraldi DA, Hiltner A, Baer E. J Polym Sci Part B Polym Phys 2002;40:862.
[3] Sherman SC, Iretskii AV, White MG, Schiraldi DA. Chem Innov 2000; 30:25.
[4] Beer D, Ramirez E. J Text Inst 1990;4:81.
[5] Tokita M, Osada K, Watanabe J. Liq Cryst 1998;24:477.
[6] Tokita M, Takahashi T, Hayashi M, Watanabe J. Macromolecules 1996; 29:1345.
[7] Gutiérrez MCG, Karger-Kocsis J, Riekel C. Macromolecules 2002;35: 7320.
[8] Ran S, Wang Z, Burger C, Chu B, Hsiao BS. Macromolecules 2002;35: 10102.
[9] Carr PL, Nicholson TM, Ward IM. Polym Adv Technol 1997;8:592.
[10] Auriemmam F, Corradini P, Rosa De C, Gureera G, Petraccone V, Biachi R, et al. Macromolecules 1992;25:2490.
[11] Welsh GE, Blundell DJ, Windle AH. Macromolecules 1998;31:7562.
[12] Li X, Brisse F. Macromolecules 1994;27:2276.
[13] Ma H, Uchida T, Collard DM, Kumar S, Schiraldi DA. Macromolecules 2004;37:7643.
[14] Schiraldi DA, Lee JJ, Gould SAC, Occelli ML. J Ind Eng Chem 2000; 7:67.

[15] Ma H, Fiber spinning, structure and properties of poly(ethylene terephthalate-*co*-4,4′ bibenzoate) copolyester fibers. M.S. Thesis, Georgia Institute of Technology, Atlanta, GA; December 2000.
[16] Alexander LE. X-ray diffraction methods in polymer science. New York, USA: Wiley; 1969.
[17] Gupta VB, Kumar S. Textile Res J 1979;7:405.
[18] Wilchinsky ZW. Adv X-ray Anal 1963;6:231.
[19] Siesler HW. Adv Polym Sci 1984;65:1.
[20] Troughton MJ, Davies GR, Ward IM. Polymer 1989;30:58.
[21] Hutchinson IJ, Ward IM, Willis HA, Zchy V. Polymer 1980;21:55.
[22] Liang CY, Krimm S. J Mol Spectrosc 1959;3:554.
[23] Daubeny RDE, Bunn CW, Brown C. J Proc Roy Soc 1954;A226:531.
[24] Cole KC, Gu'evremont J, Ajji A, Dumoulin MM. Appl Spectrosc 1994; 48:1513.
[25] Krimm S. Adv Polym Sci 1960;2:51.
[26] Spiby P, O'Neill MA, Duckett RA, Ward IM. Polymer 1992;33:4479.
[27] Ward IM. Mechanical properties of solid polymers. New York, USA: Wiley; 1979. p. 180.
[28] Boyd ISU, Boyd RH. Macromolecules 2001;34:7219.
[29] Chen LP, Yee AF, Goetz JM, Schaefer J. Macromolecules 1998;31:5371.
[30] Maxwell AS, Ward IM, Laupretre F, Monnerie L. Polymer 1998;39:6835.
[31] Wilhelm M, Spiess HW. Macromolecules 1996;29:1088.
[32] Gabrielse W, Gaur HA, Feyen FC, Veeman WS. Macromolecules 1994; 27:5811.